

Wireless wearable wristband for continuous sweat pH monitoring

Pablo Escobedo,^e Celia E. Ramos-Lorente,^a Antonio Martínez-Olmos,^{b,d} Miguel A. Carvajal,^{b,d} Mariano Ortega-Muñoz,^{c,d} Ignacio de Orbe-Payá,^{a,d} Fernando Hernández-Mateo,^{c,d} Francisco Santoyo-González,^{c,d} Luis F. Capitán-Vallvey,^{a,d} Alberto J. Palma,^{b,d} Miguel M. Erenas^{a,d}

^a ECsens, Department of Analytical Chemistry, Faculty of Sciences, Campus Fuentenueva s/n, University of Granada, 18071-Granada, Spain

^b ECsens, Department of Electronics and Computer Technology, ETSIT C/Pta. Daniel Saucedo Aranda s/n, University of Granada, 18071-Granada, Spain.

^c Department of Organic Chemistry, Biotechnology Institute, Faculty of Sciences, Campus Fuentenueva s/n, University of Granada, 18071-Granada, Spain

^d Unit of Excellence in Chemistry applied to Biomedicine and the Environment of the University of Granada.

^e Bendable Electronics and Sensing Technologies (BEST) Group, University of Glasgow, Glasgow, G12 8QQ, UK

Abstract

Several studies have shown that the determination of pH in sweat, which is one of the most accessible body fluids, can be an indicator of health and wellness, and even be used for potential disease diagnosis. On that basis, we present herein a wearable wristband for continuous and wireless monitoring of sweat pH with potential applications in the field of personal health assessment. The developed wristband consists of two main parts: a microfluidic cloth analytical device (μ CAD) to collect continuously the sweat from skin with a color-based pH sensing area; and a readout and processing module with a digital color sensor to obtain the pH of sweat from the color changes in the μ CAD. In addition, the readout module includes a low-power Bluetooth interface to transmit the measurements in real-time to a custom-designed smartphone application. To allow continuous operation, an absorbent pad was included in the design to retire and store the sweat from the sensing area through a passive pump path. It was found that the Hue parameter (H) in the HSV color space can be related to the sweat pH and fitted to a Boltzmann equation ($R^2=0.997$). The range of use of the wristband device goes from 6 to 8, which includes the pH range of sweat, with a precision at different pH values from 3.6 to 6.0 %. Considering the typical human sweat rate, the absorbent pad allows continuous operation up to more than 1000 minutes.

Keywords: pH sensor; Sweat analysis; Microfluidic cloth analytical device (μ CAD); Wearable system; Wireless monitoring; Smartphone.

45

46 **1. Introduction**

47 Wearable technology has significantly evolved in the last years with the advent of
48 products such as smartwatches and wristbands. In particular, the use of wearables for
49 personal health assessment has fuelled the growth of these devices by enabling non-
50 invasive methods for continuous monitoring of physical activity and vital signs [1,2].
51 Not surprisingly, the wearable fitness technology market was valued at \$5.77 billion in
52 2016 and it is expected to be worth \$12.44 billion by 2022, growing at an estimated
53 compound annual growth rate (CAGR) of 13.7% from 2016 to 2022 [3]. Among the
54 different physiological parameters of interest, we must highlight the monitoring of heart
55 rate [4], blood pressure [5,6], respiration rate [7], body temperature [8] and sweat [9–
56 12]. In contrast with traditional health monitoring instruments, wearable devices have
57 some key advantages such as portability, ubiquity or ease of use, and they are able to
58 provide continuous, real-time, wireless monitoring of health conditions in a non-
59 invasive way [13–16].

60 Several studies have shown that analytes of interest in blood such as glucose,
61 lactate, urea or sodium, to name but a few, are also found in other biofluids sources such
62 as saliva, tears or sweat [17]. The main advantage of using these alternative biofluids
63 lies in their easier access, thus avoiding the need for acquiring blood samples and
64 allowing peripheral biochemical monitoring [18,19]. Sweat is particularly attractive
65 since it is one of the most accessible body fluids, and it can even be produced by on-
66 demand stimulation using techniques such as iontophoresis [20]. pH determination in
67 sweat is an indicator of health and wellness, and it can be used even for potential
68 disease diagnosis. Under normal conditions, the pH of healthy human sweat is within
69 the range from 4.5 to 7.0. Nevertheless, the pH of our sweat can vary dramatically under
70 circumstances of homeostasis dysregulation, disease, acidosis and even stress [21]. For
71 instance, cystic fibrosis patients are reported to have a higher pH (up to pH 9) than
72 normal individuals [22], and sweat pH can be also used as an indicator of metabolic
73 alkalosis [23]. In the field of sport and exercise, it is well known that the formation and
74 evaporation of sweat is the principal means of heat removal. If the sweat losses lead to a
75 body water deficit or hypohydration, the reduced volume of body fluids will contain a
76 greater concentration of sodium (Na^+) and potassium (K^+), which can cause hypertonic
77 hypovolemia [24]. Severe dehydration can lead to headache, vomiting, muscle
78 cramping, dizziness, nausea and even fainting. In this context, sweat pH can be used to
79 monitor exercise intensity and dehydration since it is associated with sodium
80 concentration [25]. On the other hand, excessive water intake can cause hyponatremia,
81 which refers to a low sodium concentration. Clinical features of symptomatic
82 hyponatremia include seizures, pulmonary edema, muscle fasciculation, disorientation,
83 mental confusion, respiratory arrest, weakness, nausea and even coma [26]. Therefore,
84 the reliable monitoring of sweat pH is crucial for health assessment and wellness
85 monitoring applications [27].

86 Different approaches for wearable sweat pH monitoring can be found in the
87 literature over the last few years. According to their sensing strategy, a number of

88 platforms draw upon optical colorimetric detection [10,28–32], while others make use
89 of electrochemical pH sensors [31,33,34] reviewed by Chung et al. [19]. In the first
90 case, the use of microfluidic devices allows the precise positioning of the reagents in a
91 specific test zone to which the sweat is guided, thus taking place the desired reaction
92 with the subsequent color change [35].

93 The study of the evolution on time of sweat both rate and composition in different
94 areas of the body has been approached in two main ways referred to passive sampling:
95 *i*) microchannel-based microfluidics that rely on deterministic capillary, the so-called
96 capillary microfluidic [36]. In this case, epidermal microfluidic systems that combine
97 channels, valves, mixers, and reservoirs, are able to capture, route, and store microliters
98 of sweat in a time-controlled manner [35]; or *ii*) porous capillary microfluidics that rely
99 on stochastic capillary flow within a network of pores (paper, cloth, thread) in which the
100 sweat is collected, and delivered to the sensing area being removed by an adsorbent
101 acting as a passive pump [25].

102 To make the system truly wearable and portable, a wireless interface is required to
103 transmit the measured data to the end user. Many systems include a Radiofrequency
104 Identification (RFID) solution, usually a Near Field Communication (NFC) link
105 [32,33,37]. This approach allows the development of passive systems by means of
106 energy harvesting from the electromagnetic field of an external reader, typically an
107 NFC-enabled smartphone. Moreover, the NFC antenna required for this design can be
108 manufactured in flexible and conformable substrates, even stretchable [31,33].
109 However, this approach is not suitable for continuous, real-time sweat monitoring, since
110 it requires that the external reader is permanently placed close to the system. To
111 overcome such limitations, other systems employ longer range wireless technologies
112 such as Wi-Fi [38,39] or Bluetooth [10,34,40].

113 In this work, we present a wearable wristband for sweat pH monitoring. As Fig. 1
114 shows, the system comprises two main parts: *i*) a custom-designed microfluidic cloth
115 analytical device (μ CAD) to collect and store the sweat that includes a color-based pH
116 sensor built by immobilization of a vinyl sulfone acidochromic dye (AD-VS) on a
117 cotton cloth; and *ii*) a miniaturized readout module to obtain the pH measurements from
118 the sensor and extra circuitry to interface with the end user. The proposed wristband
119 allows continuous monitoring of sweat pH and real-time wireless transmission of the
120 measurements to a smartphone via Bluetooth. The presented system distinguishes from
121 previous works in the same field by combining the following three main aspects: *i*) The
122 development of a novel compound covalently immobilized in cloth optimized for
123 optical pH sensing with high response speed; *ii*) The inclusion of an absorbent pad to
124 retire and store the sweat from the sensing area through a passive pump path, which
125 allows continuous operation up to more than 1000 minutes; and *iii*) The design of
126 miniaturized and low-power electronics embedded with the sensing module in a
127 compact and light-weight wristband design, which is completed by a custom-developed
128 smartphone application for real-time monitoring.

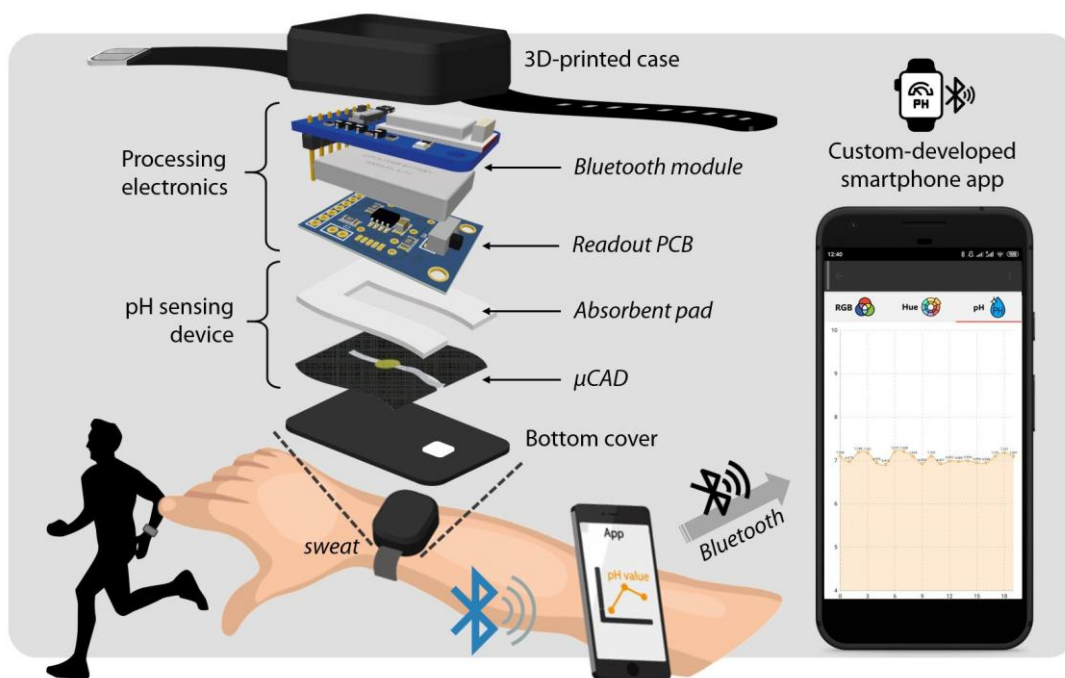


Fig. 1. Exploded view of the wireless wearable wristband, consisting of the custom-designed μ CAD with a colorimetric pH sensor and a miniaturized readout module to obtain the pH information from the sensor. Real-time measurements of sweat pH are transmitted to the user smartphone via Bluetooth through a custom-developed app.

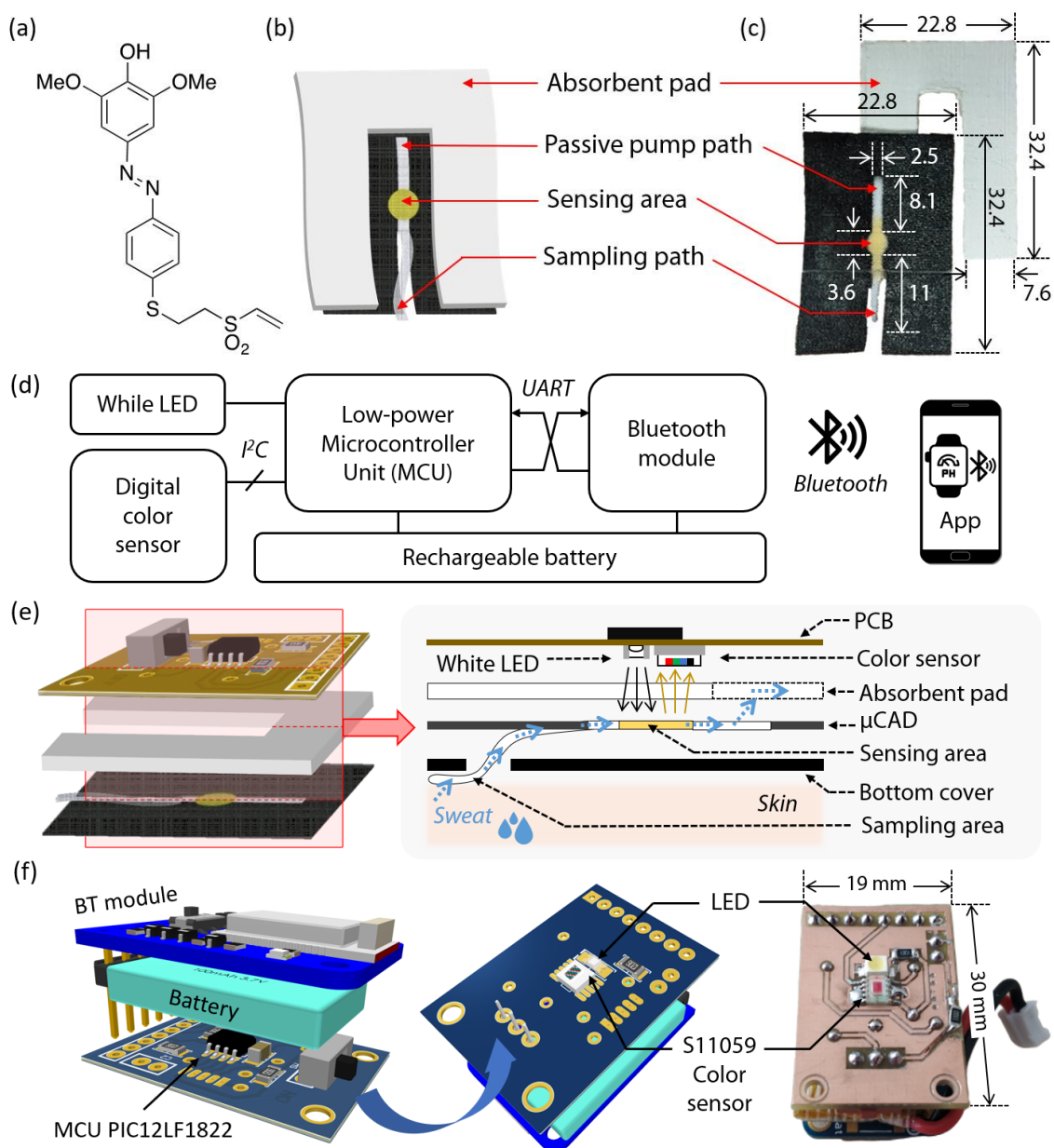
2. Materials and Methods

2.1. μ CAD design and fabrication

All reagents and materials used for the μ CAD preparation are detailed in Section S1 of the Electronic Supplementary Information (ESI), while the synthetic procedures of AD-VS-1 and its optical characterization are detailed in Sections S2 and S3, respectively. Firstly, a piece of $13.8 \times 17.4 \text{ cm}^2$ of cotton cloth, previously characterized by us in terms of Washburn constant (see Section S4), was screen-printed using a 43 lines $\cdot\text{cm}^{-1}$ frame together with a black plastisol ink, to pattern 12 hydrophilic sections as shown in Fig. S9 of Section S5. Lately, the large piece of cotton cloth was cut to obtain each pattern independently, that will be used to prepare the μ CAD. Once the cotton patterned cut was obtained, the vinyl sulfone acidochromic dye AD-VS-1 (Fig. 2(a)) was immobilized according to the following procedure. Firstly, it was introduced in a Na_2CO_3 $10 \text{ mg}\cdot\text{mL}^{-1}$ solution for 1 h to scour the screen-printed fabric and improve its capillary properties, as well as to get a basic media on the cloth that makes possible the click immobilization of the AD-VS-1 via oxa-Michael addition by adding of $0.2 \mu\text{L}$ of AD-VS-1 $15 \text{ mg}\cdot\text{mL}^{-1}$ in DMSO. Afterwards, the cloth was located in a light-safe and let dry for 24 h, and then washed to remove the excess of AD-VS-1 by sonication in Tris buffer pH=9.2, purified water and methanol, 10 minutes each. Finally, the μ CAD was placed in the bottom of the designed holder and, on top of it, the U-shaped absorbent pad as shown in Fig. 2(b-c). The μ CAD, as well as the U-shaped absorbent

158 pad, are disposable components that can be replaced when necessary. To collect the
 159 sweat, a piece of the sampling path passes through a hole at the bottom cover of the 3D-
 160 printed case, being in touch with the skin and collecting the sample while sweating.

161



162

163

164

165 **Fig. 2.** (a) Chemical structure of AD-VS-1; (b) μ CAD design; (c) μ CAD photograph; (d) Block
 166 diagram of the processing electronics in the readout module; (e) Schematic diagram of the
 167 sensing procedure in which the LED and color sensor are placed in front of the sensing area of
 168 the μ CAD; (f) 3D views and real image of the fabricated module with its main components
 169 labelled.

170

171

172

173

In humans, the rate of sweating is around $1250 \text{ g}\cdot\text{m}^{-2}\cdot\text{h}^{-1}$ when exercising [41]. For that reason, both the sampling and the sensing areas in the μ CAD design had to be small enough to avoid the need of high volumes of sample. On the other hand, however, the

174 sensing area needed to have a minimum diameter of 3.6 mm so that the detector
175 included in the device could perform reliable measurements. Cotton cloth was selected
176 as the support for the μ CAD because it presents better properties than paper in terms of
177 flexibility and bending resistance. However, as it occurs with paper, the cotton cloth
178 needed to be patterned to achieve that the sample and reagent flow through a specific
179 path. For this reason, the designed pattern (Fig. 2) comprises of several parts: (i) a
180 sampling zone where the sweat is recollected or added, (ii) a sensing area where the AD-
181 VS-1 is immobilized, and (iii) a passive pump path in which the sample flows to reach
182 (iv) an absorbent U-shaped material that makes it possible the use for a prolonged
183 operation.

184 Before the optimization of the μ CAD preparation, the analytical parameter used to
185 characterize the color change of the immobilized AD-VS-1 was selected. For this
186 purpose, several small cotton pieces were prepared as described in Section S6 and tested
187 on pH solutions ranging from 4 to 9 ($n=3$), recording and analysing the color in the RGB
188 and HSV color spaces (see Fig. S11). The Hue (H) parameter showed a higher color
189 variation at lower pH with lower error bars reason by that was used for the study (see
190 Fig. S12).

191 Once H was selected as analytical parameter and the μ CAD was designed and
192 fabricated, different parameters related to the immobilization of the AD-VS-1 were
193 studied. Firstly, the volume that must be added to the sensing area was evaluated in
194 order to cover the circle in a reproducible way. For this purpose, different volumes
195 ranging from 0.1 to 0.5 μ L of a Brilliant Blue solution ($10 \text{ mg}\cdot\text{mL}^{-1}$) were added, being
196 0.3 μ L the volume that best and most homogeneously covered the sensing area (see Fig.
197 S13 in Section S7). Later, and based on the obtained results, the same test was
198 performed using a $10 \text{ mg}\cdot\text{mL}^{-1}$ AD-VS-1 in DMSO solution to confirm these results. In
199 this case, the volume that best covered the sensing area was 0.2 μ L. The volume needed
200 in this case was lower due to the used solvent, since Brilliant Blue solution was solved
201 in water, while AD-VS was in DMSO and it affected to the wicking on cloth.

202 Later, the concentration of AD-VS-1 solution in DMSO was optimized. For this
203 purpose, different AD-VS-1 solutions from 5 to 20 $\text{mg}\cdot\text{mL}^{-1}$ (see Section S7) were
204 tested, resulting that $15 \text{ mg}\cdot\text{mL}^{-1}$ was the concentration that best results provided in
205 terms of CV as well as pH range of variation of the signal, being the one whose H value
206 changed at lower pH (see Section S8).

207 Finally, two different procedures to prepare the μ CAD were assayed (see Section
208 S9). In the first procedure, the cloth was first patterned and later the reagent was
209 immobilized. In the second procedure, these steps were followed in reverse order. The
210 obtained results (see Fig. S15) proved that the procedure providing best results in terms
211 of reproducibility was the patterning followed by the immobilization of the AD-VS-1.

212

213 **2.2. Readout and processing electronics**

214 The readout module comprises as main electronic components a low-power
215 microcontroller unit (MCU) model PIC12LF1822 (Microchip Technology Inc.,
216 Chandler, Arizona, USA); a Bluetooth module Bluefruit Low Energy (BLE) UART

217 Friend (Adafruit, New York, USA); a high-resolution digital color detector model
218 S11059-02DT (Hamamatsu Photonics, Japan); a white excitation LED; and a
219 rechargeable battery of 3.7 V and 150 mA·h capacity model JJR/C H36-004 (Goolsky,
220 Singapore, Asia). Fig. 2(d) shows the block diagram of the processing electronics.

221 The sensing module, which comprises of the excitation LED and the color detector,
222 is placed aligned in front of the pH-sensitive membrane, as shown in Fig. 2(e). The
223 selected color detector S11059-02DT is sensitive to red ($\lambda_{\text{peak}}=615$ nm), green (λ_{peak}
224 $=530$ nm), blue ($\lambda_{\text{peak}} =460$ nm), and near infrared ($\lambda_{\text{peak}} =855$ nm) incident radiation,
225 codifying it in four 16-bit digital words. These words are sent to the MCU by means of
226 an I²C interface for further processing. The excitation LED is synchronised with the
227 reading protocol of the color detector. The selected LED is white since the parameter to
228 be determined is the color of the sensitive membrane. After the processing, the MCU
229 sends the data to the Bluetooth module via Universal Asynchronous Receiver-
230 Transmitter (UART) protocol. The processed data is then wirelessly transmitted to a
231 mobile phone via Bluetooth. Fig. 2(f) shows the 3D views and real image of the
232 fabricated readout module.

233 A 3D-printed case was designed and composed of two pieces fitting each other and
234 manufactured with coal black polylactic acid (PLA) and polyurethane Filaflex. In this
235 way, we ensure the correct alignment and positioning of the pH sensor with respect to
236 the LED and color detector, while providing a uniform dark environment for the color
237 measurements. More details about the design and fabrication of the 3D-printed case can
238 be found in Section S10. In addition, to transmit the data in real-time from the wristband
239 to the user, a custom-designed Android™ application was developed. The application
240 takes control of the Bluetooth interface of the smartphone to communicate with the
241 Bluefruit LE module. Once the wristband is paired with the smartphone, the BLE sends
242 in real time the measured color data obtained through the color sensor (in RGB
243 coordinates) from the MCU to the app. The RGB coordinates are then converted to the
244 H value in the HSV color space. Finally, the pH values are computed from the
245 normalized H values as per the obtained calibration, and the graph is displayed on the
246 screen. The application includes a datalogger function and the results can be shared
247 through email and/or different cloud or messaging services, thus allowing the possibility
248 to connect to remote health care providers or medical experts. More details regarding
249 the development and some screen captures of the application can be found in Section
250 S11 of ESI.

251

252

253 **3. Results and Discussion**

254

255 **3.1. Selection, synthesis and characterization of the acidochromic dye indicator AD-** 256 **VS-1**

257 Parallel advances in chemical sensing and wireless communication technologies
258 have sparked the development of wireless chemical sensors. In this work, our
259 engineering design is based on the use of μ CAD as an optical sensor for the detection

260 and determination of pH as the analyte. In this respect, acidochromism evolved for the
261 sensing area of the μ CAD by means of an immobilized acidochromic indicator dye as a
262 recognition element was thought to be an adequate methodology [42]. Among the
263 different suitable dyes, our selection was based in the appealing features of vinyl
264 sulfone azo dyes (AD-VS). These compounds combine the outstanding optical
265 properties of azo chromophores with the relatively high reactivity of the vinyl sulfone
266 group (VS) [43,44]. The reactivity of the VS functional group fulfils most of the
267 essential requirements needed for covalent immobilization of the azo dye to cotton cloth
268 as the support of choice for the μ CAD fabrication: (i) a complementary reactivity with
269 the intrinsic nucleophilic OH present in cellulose that react by a Michael-type addition,
270 (ii) a high stability of the resulting ether link, (iii) it takes place in an aqueous milieu,
271 and (iv) a simplified one-step procedure that minimize the operational. On the base of
272 these outstanding features AD-VS have found application in textile chemistry [45] and
273 they also have demonstrated their value in the fabrication of devices for optical pH
274 sensing [42,46–48].

275 Considering the current state-of-the-art, we decided to prepare a novel member of
276 this family of compounds, named AD-VS-1 (Fig. 2(a)), as suitable for our purposes. We
277 envisaged an easy strategy based in a straightforward two-step procedure that starts
278 from 4-aminothiophenol (see Section S2). After treatment of this aromatic compound
279 with divinyl sulfone, that led exclusively to the corresponding thia-Michael reaction
280 addition intermediate due to the higher nucleophilicity of the sulfur atom respecting to
281 the amino group, concomitant diazotation reaction with 2,6-dimethoxyphenol afforded the
282 desired AD-VS-1. Spectroscopic characterization of this indicator dye confirms this
283 molecular structure, whose optical profile (absorbance spectra and molar extinction
284 coefficient in DMSO solution) was also determined (see Section S3).

285

286 **3.2. μ CAD and pH sensor performance**

287 As can be observed in Fig. 2(b-c), the hydrophilic section of the μ CAD is composed
288 by a sensing area and two paths: the sampling path (2.5 mm x 11.0 mm) and the passive
289 pump path (2.5 mm x 8.1 mm). A 2.5-mm wide path was selected since it was the
290 narrowest path that could be screen-printed on the cloth in the reproducible way. The
291 length of both paths, sensing area size, and position in the 22.8 mm x 32.4 mm piece of
292 cloth used to fabricate the μ CAD, were selected based on the Printed Circuit Board
293 (PCB) and 3D-printed case design.

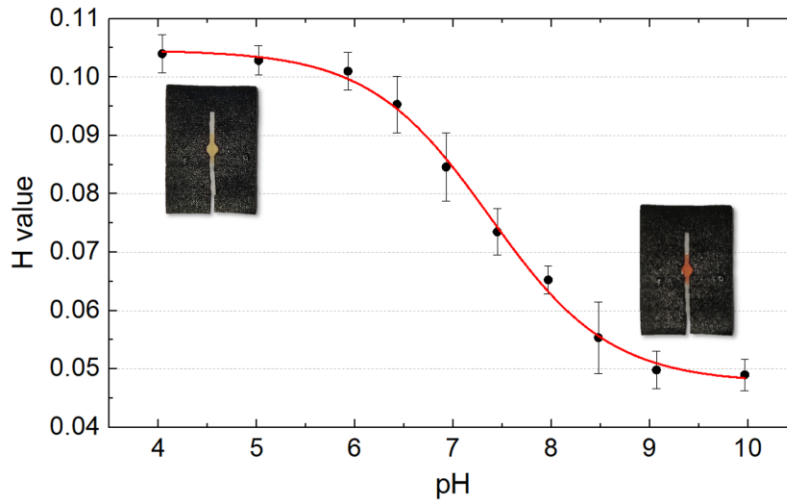
294 After the μ CAD design and optimization, a calibration was conducted by dipping
295 the μ CADs in 10 different standard solutions with pH from 4 to 10 during 30 s in each
296 solution (see Section S12). Six different μ CAD were used for the calibration. In three of
297 them, the calibration was conducted by rising the pH value of the standard solution,
298 while in the other three cases the pH was diminished during the calibration. This
299 strategy was chosen to prove that the obtained H value was independent from the pH
300 variation direction. As it can be observed in Fig. S18, the obtained results were

301 independent from the rising or diminishing of the pH value, so the six replicates were
302 used to obtain a Boltzmann equation fitting the data set ($R^2=0.997$) (see Fig. S19).

303 The results of this first study indicate that the designed μ CAD can be used to
304 determine the pH of sweat with good precision and within the range of the sample.
305 However, at this stage it cannot be claimed yet that the μ CAD could be used for real-
306 time determination of pH sweat. The reason behind this is that the μ CAD hydrophilic
307 area is so small that it will be full of sample in a very short period of time. Because of
308 that, some material needed to be included for the purpose of continuously retiring
309 sample from the hydrophilic area of the μ CAD to allow that new sample could continue
310 flowing through it. This would ensure that the μ CAD could be used during longer
311 periods of time before saturating. The strategy followed was the inclusion of a passive
312 pump in the μ CAD, along with an absorbent pad containing Flexicel (P&G Spain,
313 Madrid) skirting the hydrophilic area (see Fig. 2(b-c)). Flexicel is a superabsorbent
314 material whose characterization is shown in Section S13. According to the slope of the
315 calibration function in Fig. S20(a), this material can absorb around 20 times its weight.
316 This material has been successfully used as passive pump in other microfluidic devices
317 that can be found in the literature [49]. The area of the absorbent pad used in our design
318 was 689 mm^2 . Based on the calibration of the material and considering a sweat rate of
319 $0.01 \mu\text{L}\cdot\text{s}^{-1}$ (in around 15 mm^2 area) [41], the μ CAD along with the absorbent pad could
320 be used continuously up to 1058 min. Size and shape of the absorbent material was
321 selected based on the 3D-printed case, to be easy-to-place inside while maintaining its
322 position inside during the use of the device.

323 A new calibration was conducted, on this occasion with the μ CAD including the
324 passive pump. In this case, a syringe pump was used to apply the sample on the
325 sampling zone (see Fig. 2(b)) at a flow rate similar to the human sweat rate ($0.01 \mu\text{L}\cdot\text{s}^{-1}$).
326 Each pH standard solution was applied to the μ CAD during two minutes and
327 videotaped. From the obtained results (see Fig. S21 in Section S14) it can be observed
328 that only 90 seconds were enough to get a steady signal, which was used to obtain the
329 calibration function (see Fig. 3). The data fits as previously described to a Boltzmann
330 equation ($R^2=0.996$) (Eq. S2), and the range of use of the μ CAD is from 6.1 to 8.4
331 ($\text{pK}_a=7.4$), range in which the pH of sweat is included. The precision tested at different
332 pH goes from 2.3 to 3.6 % (see Table 1).

333



334
 335 **Fig. 3.** Calibration curve of the μ CAD including the passive pump, where the standard pH
 336 solutions were applied on the sampling zone using a syringe pump at a rate of $0.01 \mu\text{L}\cdot\text{s}^{-1}$,
 337 which is similar to the human sweat rate.
 338

339
 340 **Table 1.** Analytical parameters of μ CAD.

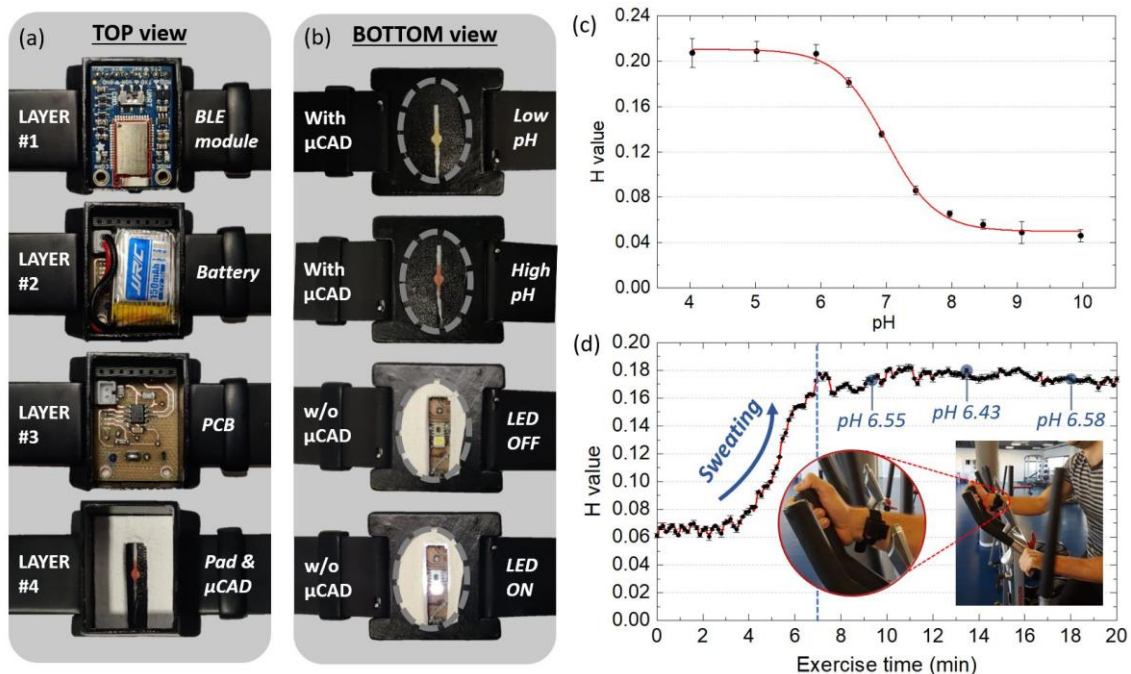
Analytical parameters			
A_1	0.104	Precision (n=10)	
A_2	0.047	pH	CV (%)
A_3	7.372		
A_4	0.614	4.04	2.5
R^2	0.996	7.45	3.5
LOD	6.1	7.97	2.3
Range	6.1 - 8.4	9.97	3.6

341
 342
 343
 344
 345
 346
 347
 348
 349
 350
 351 Due to the nature of the sweat sample, whose pH can rise or diminish indistinctly
 352 during an exercise session, an additional study was conducted (see Section S14) to
 353 prove that the μ CAD is fully reversible to pH variations. Fig. S22 shows that the
 354 μ CADs are fully reversible after subjecting them to a cycle of acidic-basic-acidic pH
 355 and basic-acidic-basic pH, respectively. Finally, a stability study included in Section
 356 S15 was performed by observing the H value of three different μ CADs along 20 weeks.
 357 This study showed that, once prepared, the μ CAD can be stored for 7 weeks (Fig. S23).
 358 Once the μ CAD was fully characterized, seven different samples were analysed using
 359 the μ CAD and the obtained results were compared to the ones provided by a pH-meter
 360 (Section S16).
 361

362 **3.3. Wristband performance and evaluation**

363
 364 As indicated in the previous section, the μ CAD was analytically characterized for pH
 365 sensing and a calibration function was obtained using a camera to register the color
 366 variations (see Fig. 3). At this stage, the whole system was characterized using the

367 optimized μ CAD in combination with the readout and processing electronics. Thus, the
 368 way of registering the color changes in the μ CAD due to the sweat pH was conducted
 369 through the digital color sensor included in the readout circuit (see Fig. 4(a-b)). For the
 370 calibration, a similar setup than the previous case was employed, i.e. a syringe pump
 371 was used to apply the sample on the sampling zone at a flow rate similar to the human
 372 sweat rate ($0.01 \mu\text{L}\cdot\text{s}^{-1}$). Each pH standard solution was applied to the μ CAD during
 373 two minutes and the color measurements from the digital sensor were transmitted every
 374 second to the smartphone app via Bluetooth. Fig. 4(c) shows the obtained calibration
 375 curve, that can be again fitted to a Boltzmann curve ($R^2=0.997$) (Eq. S2). In this case,
 376 the range of use of the μ CAD ranges from 6.0 to 8.0, and the precision at different pH
 377 values goes from 3.6 to 6.0 % (see Table 2). In addition, the system was tested in real-
 378 life conditions by wearing it on the wrist while exercising and transmitting the data in
 379 real-time to a smartphone via Bluetooth. Fig. 4(d) shows the experimental setup and the
 380 obtained results. Two different sections can be distinguished in this graph: (i) a priming
 381 section (0-7 min) that comprise the time to start sweating as well as wetting the fluidic
 382 channel and sensing area; and (ii) a pH-responsive section once the whole system is
 383 conditioned. Once the priming time has finished (vertical dashed line in Fig. 4(d)) the
 384 sampling area has changed its color due to the sweat pH. Considering the device
 385 calibration depicted in Fig. 4(c), which was conducted using pH standard solutions, we
 386 have highlighted in Fig. 4(d) some pH values in this section. At that point, the pH
 387 values stand at around 6.4 – 6.6, which is consistent with previous research works in
 388 this field [34,51].
 389



390
 391 **Fig. 4.** (a) Layer by layer top view of the wristband, including: 1) Low-Energy Bluetooth
 392 module, 2) battery, 3) PCB, and 4) absorbent pad with μ CAD; (b) Bottom view of the wristband
 393 (uncovered) with and without the μ CAD layer to allow the view of the LED and color detector;
 394 (c) Calibration curve of the wristband wearable system in terms of H value; (d) Real-time
 395 results of the wearable system placed on the wristband during exercise.

396
397
398
399
400
401
402
403
404
405

Table 2. Analytical parameters of the wristband.

Analytical parameters			
A₁	0.210	Precision (n=10)	
A₂	0.050	pH	CV (%)
A₃	0.699	6.00	4.0
A₄	0.377	6.43	6.0
R²	0.997	6.93	4.5
LOD	6.0	7.45	4.3
Range	6.0 - 8.0	7.97	3.6

406
407
408
409
410
411
412
413
414
415
416
417
418
419
420
421
422
423
424
425
426
427
428
429
430

Overall, the developed system is convenient in terms of portability, ease of use and wearability. With a total weight of 25 g (including the strap), which is in line with the most popular fitness wristbands such as the Fitbit Charge 4 (30 g), Garmin Vivosport (27 g), or Samsung Galaxy Fit (24 g), the developed wristband is light-weight and comfortable to wear. A number of previous works have focused on the development of sensing patches for sweat pH monitoring [18,25,28,30,52], but they lacked the associated readout and processing electronics to obtain and transmit in real-time the measured information to the end user. In contrast to the RFID/NFC-based platforms for pH sweat sensing than can be found in previous literature [15,31,37], our proposed wristband does not require that the external reader is permanently placed in its close proximity, thus allowing a truly continuous real-time monitoring. In return, our system requires a battery for its operation, which is not needed in the case of RFID/NFC devices with energy harvesting capabilities [33]. However, the use of low-power components in combination with the non-continuous measurement strategy allows a long battery life of more than 2 days. More details regarding the electronics performance and battery life can be found in Section S17. In terms of response speed, our system only takes 90 seconds to get a steady signal in the sensing zone through the use of the passive pump to collect the sweat, which is significantly lower than the time required in other systems to get the first readings [9]. Besides, the proposed wristband is distinguished from previous sweat pH monitoring systems in two more aspects: firstly, it features a very compact and light-weight design with a size similar to a wristwatch, making it more comfortable to use than other devices that must be placed, for instance, in the back; and secondly, it is completed by a custom-developed user-friendly smartphone application [10,28,34,40].

431
432
433

4. Conclusions

434
435
436
437
438

A wearable wristband for sweat pH wireless monitoring was developed combining a custom-designed μ CAD and associated readout and processing electronics. The μ CAD was designed in 100% cotton cloth by immobilizing an acidochromic dye (AD-VS-1). The μ CAD consists of a sampling area to collect the sweat, a colorimetric sensing area, a passive pump path, and an absorbent pad that allows continuous operation up to 100

439 min if we consider a typical human sweat rate ($0.01 \mu\text{L}\cdot\text{s}^{-1}$). The H value in the HSV
440 color space was selected as the best parameter to correlate the color change in the
441 sensing area due to the pH variations. The readout module consists of a low-power
442 microcontroller unit that controls a white LED and a digital color sensor to detect the
443 color variations in the μCAD sensing area. In addition, a Bluetooth module transmits in
444 real-time the measurements to a friendly-user smartphone application. The analytical
445 characterization of the μCAD alone showed that the H parameter can be related to the
446 sweat pH value and fitted to a Boltzmann equation ($R^2=0.996$). The range of use of the
447 μCAD goes from 6.1 to 8.4, which includes the pH range of sweat. The precision tested
448 at different pH values goes from 2.3 to 3.6 %. When compared to a commercial pH-
449 meter with different samples, the error in the determination was around 2% in almost all
450 the cases. The analytical characterization of the wristband as a whole showed a good
451 fitting ($R^2=0.997$ in the Boltzmann equation) with a range of use from 6 to 8 and a
452 precision at different pH values from 3.6 to 6.0 %. With an estimated battery life up to
453 2.63 days in non-continuous sensing mode, the developed system has potential
454 applications in the field of personal health assessment.

455

456

457 **Declaration of interests**

458 The authors declare that they have no known competing financial interests or personal
459 relationships that could have appeared to influence the work reported in this paper.

460

461 **Acknowledgements**

462 This work was funded by Spanish “Ministerio de Economía y Competitividad” (
463 Projects PID2019-103938RB-I00 and CTQ2017-86125-P) and Junta de Andalucía
464 (Projects B-FQM-243-UGR18 and P18-RT-2961). The projects were partially
465 supported by European Regional Development Funds (ERDF).

466

467 **References**

468

- 469 [1] B.W. An, J.H. Shin, S.-Y. Kim, J. Kim, S. Ji, J. Park, Y. Lee, J. Jang, Y.-G. Park, E.
470 Cho, S. Jo, J.-U. Park, Smart Sensor Systems for Wearable Electronic Devices, *Polymers*
471 (Basel). 9 (2017) 303. doi:10.3390/polym9080303.
- 472 [2] I.C. Jeong, D. Bychkov, P.C. Searson, Wearable devices for precision medicine and
473 health state monitoring, *IEEE Trans. Biomed. Eng.* 66 (2019) 1242–1258.
474 doi:10.1109/TBME.2018.2871638.
- 475 [3] MarketsandMarkets, Wearable Fitness Technology Market, (2016).
476 [https://www.marketsandmarkets.com/Market-Reports/wearable-fitness-technology-](https://www.marketsandmarkets.com/Market-Reports/wearable-fitness-technology-market-139869705.html)
477 [market-139869705.html](https://www.marketsandmarkets.com/Market-Reports/wearable-fitness-technology-market-139869705.html).
- 478 [4] P.J. Chacon, L. Pu, T.H. da Costa, Y.H. Shin, T. Ghomian, H. Shamkhalichenar, H.C.
479 Wu, B.A. Irving, J.W. Choi, A Wearable Pulse Oximeter with Wireless Communication
480 and Motion Artifact Tailoring for Continuous Use, *IEEE Trans. Biomed. Eng.* 66 (2018)
481 1505–1513. doi:10.1109/TBME.2018.2874885.
- 482 [5] C.M. Boutry, L. Beker, Y. Kaizawa, C. Vassos, H. Tran, A.C. Hinckley, R. Pfattner, S.
483 Niu, J. Li, J. Claverie, Z. Wang, J. Chang, P.M. Fox, Z. Bao, Biodegradable and flexible
484 arterial-pulse sensor for the wireless monitoring of blood flow, *Nat. Biomed. Eng.* 3
485 (2019) 47–57. doi:10.1038/s41551-018-0336-5.

- 486 [6] F. Riaz, M.A. Azad, J. Arshad, M. Imran, A. Hassan, S. Rehman, Pervasive blood
487 pressure monitoring using Photoplethysmogram (PPG) sensor, *Futur. Gener. Comput.*
488 *Syst.* 98 (2019) 120–130. doi:10.1016/j.future.2019.02.032.
- 489 [7] F. Güder, A. Ainla, J. Redston, B. Mosadegh, A. Glavan, T.J. Martin, G.M. Whitesides,
490 Paper-Based Electrical Respiration Sensor, *Angew. Chemie Int. Ed.* 55 (2016) 5727–
491 5732. doi:10.1002/anie.201511805.
- 492 [8] M. Manas, A. Sinha, S. Sharma, M.R. Mahboob, A novel approach for IoT based
493 wearable health monitoring and messaging system, *J. Ambient Intell. Humaniz. Comput.*
494 10 (2018) 2817–2828. doi:10.1007/s12652-018-1101-z.
- 495 [9] G. Liu, C. Ho, N. Slappey, Z. Zhou, S.E. Snelgrove, M. Brown, A. Grabinski, X. Guo,
496 Y. Chen, K. Miller, J. Edwards, T. Kaya, A wearable conductivity sensor for wireless
497 real-time sweat monitoring, *Sensors Actuators B Chem.* 227 (2016) 35–42.
498 doi:10.1016/j.snb.2015.12.034.
- 499 [10] H.Y.Y. Nyein, L. Tai, Q.P. Ngo, M. Chao, G.B. Zhang, W. Gao, M. Bariya, J. Bullock,
500 H. Kim, H.M. Fahad, A. Javey, A Wearable Microfluidic Sensing Patch for Dynamic
501 Sweat Secretion Analysis, *ACS Sensors.* 3 (2018) 944–952.
502 doi:10.1021/acssensors.7b00961.
- 503 [11] W. Gao, S. Emaminejad, H.Y.Y. Nyein, S. Challa, K. Chen, A. Peck, H.M. Fahad, H.
504 Ota, H. Shiraki, D. Kiriya, D.-H. Lien, G.A. Brooks, R.W. Davis, A. Javey, Fully
505 integrated wearable sensor arrays for multiplexed in situ perspiration analysis, *Nature.*
506 529 (2016) 509–514. doi:10.1038/nature16521.
- 507 [12] A. Martín, J. Kim, J.F. Kurniawan, J.R. Sempionatto, J.R. Moreto, G. Tang, A.S.
508 Campbell, A. Shin, M.Y. Lee, X. Liu, J. Wang, Epidermal Microfluidic Electrochemical
509 Detection System: Enhanced Sweat Sampling and Metabolite Detection, *ACS Sensors.* 2
510 (2017) 1860–1868. doi:10.1021/acssensors.7b00729.
- 511 [13] M. Parrilla, T. Guinovart, J. Ferré, P. Blondeau, F.J. Andrade, A Wearable Paper- Based
512 Sweat Sensor for Human Perspiration Monitoring, *Adv. Healthc. Mater.* 8 (2019)
513 1900342. doi:10.1002/adhm.201900342.
- 514 [14] W. Gao, H. Ota, D. Kiriya, K. Takei, A. Javey, Flexible Electronics toward Wearable
515 Sensing, *Acc. Chem. Res.* 52 (2019) 523–533. doi:10.1021/acs.accounts.8b00500.
- 516 [15] G. Xu, C. Cheng, Z. Liu, W. Yuan, X. Wu, Y. Lu, S.S. Low, J. Liu, L. Zhu, D. Ji, S. Li,
517 Z. Chen, L. Wang, Q. Yang, Z. Cui, Q. Liu, Battery- Free and Wireless Epidermal
518 Electrochemical System with All- Printed Stretchable Electrode Array for Multiplexed
519 In Situ Sweat Analysis, *Adv. Mater. Technol.* 4 (2019) 1800658.
520 doi:10.1002/admt.201800658.
- 521 [16] L. Ortega, A. Llorella, J.P. Esquivel, N. Sabaté, Self-powered smart patch for sweat
522 conductivity monitoring, *Microsystems Nanoeng.* 5 (2019) 3. doi:10.1038/s41378-018-
523 0043-0.
- 524 [17] J. Heikenfeld, A. Jajack, B. Feldman, S.W. Granger, S. Gaitonde, G. Begtrup, B.A.
525 Katchman, Accessing analytes in biofluids for peripheral biochemical monitoring, *Nat.*
526 *Biotechnol.* 37 (2019) 407–419. doi:10.1038/s41587-019-0040-3.
- 527 [18] F.J. Zhao, M. Bonmarin, Z.C. Chen, M. Larson, D. Fay, D. Runnoe, J. Heikenfeld, Ultra-
528 simple wearable local sweat volume monitoring patch based on swellable hydrogels, *Lab*
529 *Chip.* 20 (2020) 168–174. doi:10.1039/C9LC00911F.
- 530 [19] M. Chung, G. Fortunato, N. Radacsi, Wearable flexible sweat sensors for healthcare
531 monitoring: A review, *J. R. Soc. Interface.* 16 (2019). doi:10.1098/rsif.2019.0217.
- 532 [20] J. Kim, J.R. Sempionatto, S. Imani, M.C. Hartel, A. Barfidokht, G. Tang, A.S. Campbell,
533 P.P. Mercier, J. Wang, Simultaneous Monitoring of Sweat and Interstitial Fluid Using a
534 Single Wearable Biosensor Platform, *Adv. Sci.* 5 (2018). doi:10.1002/advs.201800880.
- 535 [21] T.S. Perry, Wearable sensor detects stress in sweat, *IEEE Spectr.* 55 (2018) 14–15.
536 doi:10.1109/MSPEC.2018.8449037.
- 537 [22] W.P. Nikolajek, H.M. Emrich, pH of sweat of patients with cystic fibrosis, *Klin.*
538 *Wochenschr.* 54 (1976) 287–288. doi:10.1007/BF01468925.
- 539 [23] M.J. Patterson, S.D.R. Galloway, M.A. Nimmo, Effect of induced metabolic alkalosis on
540 sweat composition in men, *Acta Physiol. Scand.* 174 (2002) 41–46. doi:10.1046/j.1365-

- 541 201x.2002.00927.x.
- 542 [24] M.N. Sawka, E.F. Coyle, Influence of Body Water and Blood Volume on
543 Thermoregulation and Exercise Performance in the Heat, *Exerc. Sport Sci. Rev.* 27
544 (1999) 167–218. doi:10.1249/00003677-199900270-00008.
- 545 [25] V.F. Curto, C. Fay, S. Coyle, R. Byrne, C. O’Toole, C. Barry, S. Hughes, N. Moyna, D.
546 Diamond, F. Benito-Lopez, Real-time sweat pH monitoring based on a wearable
547 chemical barcode micro-fluidic platform incorporating ionic liquids, *Sensors Actuators*
548 *B Chem.* 171–172 (2012) 1327–1334. doi:10.1016/j.snb.2012.06.048.
- 549 [26] T.D. Noakes, The hyponatremia of exercise., *Int. J. Sport Nutr.* 2 (1992) 205–228.
- 550 [27] T. Kaya, G. Liu, J. Ho, K. Yelamarthi, K. Miller, J. Edwards, A. Stannard, Wearable
551 Sweat Sensors: Background and Current Trends, *Electroanalysis.* 31 (2019) 411–421.
552 doi:10.1002/elan.201800677.
- 553 [28] D. Morris, S. Coyle, Y. Wu, K.T. Lau, G. Wallace, D. Diamond, Bio-sensing textile
554 based patch with integrated optical detection system for sweat monitoring, *Sensors*
555 *Actuators B Chem.* 139 (2009) 231–236. doi:10.1016/j.snb.2009.02.032.
- 556 [29] N. Lopez-Ruiz, V.F. Curto, M.M.M. Erenas, F. Benito-Lopez, D. Diamond, A.J. Palma,
557 L.F. Capitan-Vallvey, Smartphone-Based Simultaneous pH and Nitrite Colorimetric
558 Determination for Paper Microfluidic Devices, *Anal. Chem.* 86 (2014) 9554–9562.
559 doi:10.1021/ac5019205.
- 560 [30] X. He, T. Xu, Z. Gu, W. Gao, L.-P. Xu, T. Pan, X. Zhang, Flexible and Superwetable
561 Bands as a Platform toward Sweat Sampling and Sensing, *Anal. Chem.* 91 (2019) 4296–
562 4300. doi:10.1021/acs.analchem.8b05875.
- 563 [31] A.J. Bandodkar, P. Gutruf, J. Choi, K. Lee, Y. Sekine, J.T. Reeder, W.J. Jeang, A.J.
564 Aranyosi, S.P. Lee, J.B. Model, R. Ghaffari, C.-J. Su, J.P. Leshock, T. Ray, A. Verrillo,
565 K. Thomas, V. Krishnamurthi, S. Han, J. Kim, S. Krishnan, T. Hang, J.A. Rogers,
566 Battery-free, skin-interfaced microfluidic/electronic systems for simultaneous
567 electrochemical, colorimetric, and volumetric analysis of sweat, *Sci. Adv.* 5 (2019)
568 eaav3294. doi:10.1126/sciadv.aav3294.
- 569 [32] A. Koh, D. Kang, Y. Xue, S. Lee, R.M. Pielak, J. Kim, T. Hwang, S. Min, A. Banks, P.
570 Bastien, M.C. Manco, L. Wang, K.R. Ammann, K.-I. Jang, P. Won, S. Han, R. Ghaffari,
571 U. Paik, M.J. Slepian, G. Balooch, Y. Huang, J.A. Rogers, A soft, wearable microfluidic
572 device for the capture, storage, and colorimetric sensing of sweat, *Sci. Transl. Med.* 8
573 (2016) 366ra165-366ra165. doi:10.1126/scitranslmed.aaf2593.
- 574 [33] W. Dang, L. Manjakkal, W.T. Navaraj, L. Lorenzelli, V. Vinciguerra, R. Dahiya,
575 Stretchable wireless system for sweat pH monitoring, *Biosens. Bioelectron.* 107 (2018)
576 192–202. doi:10.1016/j.bios.2018.02.025.
- 577 [34] S. Anastasova, B. Crewther, P. Bemnowicz, V. Curto, H.M. Ip, B. Rosa, G.-Z. Yang, A
578 wearable multisensing patch for continuous sweat monitoring, *Biosens. Bioelectron.* 93
579 (2017) 139–145. doi:10.1016/j.bios.2016.09.038.
- 580 [35] J. Choi, R. Ghaffari, L.B. Baker, J.A. Rogers, Skin-interfaced systems for sweat
581 collection and analytics, *Sci. Adv.* 4 (2018) 1–10. doi:10.1126/sciadv.aar3921.
- 582 [36] A. Olanrewaju, M. Beaugrand, M. Yafia, D. Juncker, Capillary microfluidics in
583 microchannels: from microfluidic networks to capillary circuits, *Lab Chip.* 18 (2018)
584 2323–2347. doi:10.1039/C8LC00458G.
- 585 [37] M. Boada, A. Lazaro, R. Villarino, D. Girbau, Battery-Less NFC Sensor for pH
586 Monitoring, *IEEE Access.* 7 (2019) 33226–33239. doi:10.1109/ACCESS.2019.2904109.
- 587 [38] Y. Lu, K. Jiang, D. Chen, G. Shen, Wearable sweat monitoring system with integrated
588 micro-supercapacitors, *Nano Energy.* 58 (2019) 624–632.
589 doi:10.1016/j.nanoen.2019.01.084.
- 590 [39] R. Kansara, P. Bhojani, J. Chauhan, Designing Smart Wearable to measure Health
591 Parameters, in: 2018 Int. Conf. Smart City Emerg. Technol., IEEE, 2018: pp. 1–5.
592 doi:10.1109/ICSCET.2018.8537314.
- 593 [40] A. Alizadeh, A. Burns, R. Lenigk, R. Gettings, J. Ashe, A. Porter, M. McCaul, R.
594 Barrett, D. Diamond, P. White, P. Skeath, M. Tomczak, A wearable patch for continuous
595 monitoring of sweat electrolytes during exertion, *Lab Chip.* 18 (2018) 2632–2641.

- 596 doi:10.1039/c8lc00510a.
- 597 [41] S.F. Godek, A.R. Bartolozzi, R. Burkholder, E. Sugarman, C. Peduzzi, Sweat Rates and
598 Fluid Turnover in Professional Football Players: A Comparison of National Football
599 League Linemen and Backs, *J. Athl. Train.* 43 (2008) 184–189. doi:10.4085/1062-6050-
600 43.2.184.
- 601 [42] G.J. Mohr, H. Müller, B. Bussemer, A. Stark, T. Carofiglio, S. Trupp, R. Heuermann, T.
602 Henkel, D. Escudero, L. González, Design of acidochromic dyes for facile preparation of
603 pH sensor layers, *Anal. Bioanal. Chem.* 392 (2008) 1411–1418. doi:10.1007/s00216-
604 008-2428-7.
- 605 [43] J. Morales-Sanfrutos, J. Lopez-Jaramillo, M. Ortega-Muñoz, A. Megia-Fernandez, F.
606 Perez-Balderas, F. Hernandez-Mateo, F. Santoyo-Gonzalez, Vinyl sulfone: a versatile
607 function for simple bioconjugation and immobilization, *Org. Biomol. Chem.* 8 (2010)
608 667–675. doi:10.1039/B920576D.
- 609 [44] F.J. López-Jaramillo, F. Hernández-Mateo, F. Santoyo-González, Vinyl Sulfone: A
610 Multi-Purpose Function in Proteomics, in: *Integr. Proteomics, InTech*, 2012.
611 doi:10.5772/29682.
- 612 [45] G.J. Mohr, Synthesis of naphthalimide-based indicator dyes with a 2-
613 hydroxyethylsulfonyl function for covalent immobilisation to cellulose, *Sensors*
614 *Actuators B Chem.* 275 (2018) 439–445. doi:10.1016/j.snb.2018.07.095.
- 615 [46] T. Werner, O.S. Wolfbeis, Optical sensor for the pH 10-13 range using a new support
616 material, *Fresenius. J. Anal. Chem.* 346 (1993) 564–568. doi:10.1007/BF00321245.
- 617 [47] P. Kassal, M. Zubak, G. Scheipl, G.J. Mohr, M.D. Steinberg, I. Murković Steinberg,
618 Smart bandage with wireless connectivity for optical monitoring of pH, *Sensors*
619 *Actuators B Chem.* 246 (2017) 455–460. doi:10.1016/j.snb.2017.02.095.
- 620 [48] P. Chauhan, C. Hadad, A.H. López, S. Silvestrini, V. La Parola, E. Frison, M. Maggini,
621 M. Prato, T. Carofiglio, A nanocellulose–dye conjugate for multi-format optical pH-
622 sensing, *Chem. Commun.* 50 (2014) 9493–9496. doi:10.1039/C4CC02983F.
- 623 [49] W.T. Suarez, M.O.K. Franco, L.F. Capitán-Vallvey, M.M. Erenas, Chitosan-modified
624 cotton thread for the preconcentration and colorimetric trace determination of Co(II),
625 *Microchem. J.* 158 (2020) 105137. doi:10.1016/j.microc.2020.105137.
- 626 [50] S. Coyle, D. Morris, K.-T. Lau, D. Diamond, F. Di Francesco, N. Taccini, M.G. Trivella,
627 D. Costanzo, P. Salvo, J.-A. Porchet, J. Luprano, Textile sensors to measure sweat pH
628 and sweat-rate during exercise, in: *Proc. 3d Int. ICST Conf. Pervasive Comput. Technol.*
629 *Healthc., ICST, 2009.* doi:10.4108/ICST.PERVASIVEHEALTH2009.5957.
- 630 [51] M. Caldara, C. Colleoni, E. Guido, V. Re, G. Rosace, Optical monitoring of sweat pH by
631 a textile fabric wearable sensor based on covalently bonded litmus-3-
632 glycidoxypopyltrimethoxysilane coating, *Sensors Actuators B Chem.* 222 (2016) 213–
633 220. doi:10.1016/j.snb.2015.08.073.
- 634 [52] A. Koh, D. Kang, Y. Xue, S. Lee, R.M. Pielak, J. Kim, T. Hwang, S. Min, A. Banks, P.
635 Bastien, M.C. Manco, L. Wang, K.R. Ammann, K.-I. Jang, P. Won, S. Han, R. Ghaffari,
636 U. Paik, M.J. Slepian, G. Balooch, Y. Huang, J.A. Rogers, A soft, wearable microfluidic
637 device for the capture, storage, and colorimetric sensing of sweat, *Sci. Transl. Med.* 8
638 (2016) 366ra165-366ra165. doi:10.1126/scitranslmed.aaf2593.
- 639